

Tribological Properties of the Fast Ceramic Conversion Treated Ti-6Al-2Sn-4Zr-2Mo Alloy with a Pre-Deposited Gold Layer

Zhang, Zhenxue; Xiao, Yue; Liu, Chen; Dong, Hanshan

DOI:

[10.3390/lubricants12040105](https://doi.org/10.3390/lubricants12040105)

License:

Creative Commons: Attribution (CC BY)

Document Version

Publisher's PDF, also known as Version of record

Citation for published version (Harvard):

Zhang, Z, Xiao, Y, Liu, C & Dong, H 2024, 'Tribological Properties of the Fast Ceramic Conversion Treated Ti-6Al-2Sn-4Zr-2Mo Alloy with a Pre-Deposited Gold Layer', *Lubricants*, vol. 12, no. 4, 105.
<https://doi.org/10.3390/lubricants12040105>

[Link to publication on Research at Birmingham portal](#)

General rights

Unless a licence is specified above, all rights (including copyright and moral rights) in this document are retained by the authors and/or the copyright holders. The express permission of the copyright holder must be obtained for any use of this material other than for purposes permitted by law.

- Users may freely distribute the URL that is used to identify this publication.
- Users may download and/or print one copy of the publication from the University of Birmingham research portal for the purpose of private study or non-commercial research.
- User may use extracts from the document in line with the concept of 'fair dealing' under the Copyright, Designs and Patents Act 1988 (?)
- Users may not further distribute the material nor use it for the purposes of commercial gain.

Where a licence is displayed above, please note the terms and conditions of the licence govern your use of this document.

When citing, please reference the published version.



Take down policy

While the University of Birmingham exercises care and attention in making items available there are rare occasions when an item has been uploaded in error or has been deemed to be commercially or otherwise sensitive.

If you believe that this is the case for this document, please contact UBIRA@lists.bham.ac.uk providing details and we will remove access to the work immediately and investigate.

Article

Tribological Properties of the Fast Ceramic Conversion Treated Ti-6Al-2Sn-4Zr-2Mo Alloy with a Pre-Deposited Gold Layer

Zhenxue Zhang , Yue Xiao, Chen Liu and Hanshan Dong 

School of Metallurgy and Materials, The University of Birmingham, Birmingham B15 2TT, UK; h.dong.20@bham.ac.uk (H.D.)

* Correspondence: z.zhang.1@bham.ac.uk

Abstract: Ceramic conversion treatment (CCT) is an effective way to modify the surface of titanium alloys. However, this process normally needs more than a 100-h treatment at 600–700 °C to form a hard and wear-resistant titanium oxide layer. In this paper, we pre-deposited a thin gold layer on the surface of Ti-6Al-2Sn-4Zr-2Mo (Ti6242) samples before CCT to investigate if Au can speed up the treatment. Treatments at 640/670/700 °C were carried out for 10 or 120 h. After CCT, the surface roughness, surface morphology, microstructure, elemental composition, and phase constituents were characterized. Surface hardness and the nano-hardness depth distribution were measured. Finally, reciprocating sliding tribological tests were carried out to study the friction and wear of the surface layers. Thin gold layers accelerated the CCT significantly with a much thicker oxide layer. The friction of the untreated Ti6242 alloy against the WC ball was unsteady and high, but it was much lower and stable for the CCTed samples pre-deposited with Au because of the formation of titanium oxides and lubrication effect of the gold particles. The wear resistance of the CCTed Ti6242 alloy samples with gold was reinforced significantly. By pre-depositing a thin gold layer on the surface of Ti6242, the treatment time can be cut significantly, and CCT becomes more efficient.

Keywords: ceramic conversion treatment; Ti-6Al-2Sn-4Zr-2Mo; friction; wear; gold



Citation: Zhang, Z.; Xiao, Y.; Liu, C.; Dong, H. Tribological Properties of the Fast Ceramic Conversion Treated Ti-6Al-2Sn-4Zr-2Mo Alloy with a Pre-Deposited Gold Layer. *Lubricants* **2024**, *12*, 105. <https://doi.org/10.3390/lubricants12040105>

Received: 19 February 2024

Revised: 15 March 2024

Accepted: 21 March 2024

Published: 23 March 2024



Copyright: © 2024 by the authors. Licensee MDPI, Basel, Switzerland. This article is an open access article distributed under the terms and conditions of the Creative Commons Attribution (CC BY) license (<https://creativecommons.org/licenses/by/4.0/>).

1. Introduction

Ti-6Al-2Sn-4Zr-2Mo (Ti6242) is a weldable, near-alpha titanium alloy. Aluminum is an active α -stabilizing element, while tin works with aluminum for solution strengthening. Zirconium is also a solid solution strengthener with a neutral influence on stabilizing phases, while molybdenum is a premier β -stabilizing element to lower the β -transus temperature [1]. Ti6242 alloys offer high tensile and toughness properties and exceptional resistance to corrosion, fatigue, and creep to temperatures as high as 550 °C [2]. The materials are used extensively in high-tech industries like aerospace and motorsport with applications including gas turbine components such as turbines, discs, impellers, and precision racing engine parts [3,4]. However, titanium and its alloys have relatively low hardness and easily cause seizure in service, and severe adhesive wear and unsteady friction limit their applications under load [5]. Various surface modification and coating techniques have been used to reinforce the tribological properties of the titanium alloys, for example, shot peening [6], thermal spraying [7], plasma nitriding [8], physical vapor deposition (PVD) [9], chemical vapor deposition (CVD) [10], ion implantation [11], laser surface modification [12], etc. [13,14]. Oxygen as an alpha stabilizer and a strong interstitial strengthening element enables its' role in modifying the surface. Anodic oxidation uses electrolytes (i.e., sulfuric acid, phosphoric acid, and others) to prepare oxide films on the surface of the anode titanium alloys. The electric field-driven anodic oxidation promotes the diffusion of metal ions and oxygen ions, resulting in enhanced adhesion and wear resistance [15,16]. However, the oxide film formed is often nonuniform and porous. Plasma electrolytic oxidation (PEO) can produce oxide ceramic-like coatings on metal substrates

submerged in electrolytes to obtain coatings with high hardness and excellent corrosion and abrasion resistance. The surface is rough with a two-layer structure and defects, and normally, further treatment, like laser processing, is needed [17]. As an environmentally friendly and low-cost technique, ceramic conversion treatment (CCT) aims to improve the tribological performance of titanium alloys by obtaining a thin and compact oxide layer backed by an oxygen diffusion zone [18]. However, this process normally needs more than 100 h of treatment at 600–700 °C to form a hard and wear-resistant titanium oxide layer. Recently, we developed a fast CCT by pre-depositing a metal layer like gold or silver to accelerate the CCT of commercial pure titanium (CPTi) and Ti6Al4V to shorten the treatment time to a few hours to save energy [19,20]. Thanks to its frictional properties and long-term stability, gold is well-known as one of the most encouraging solid lubricants [21]. Furthermore, gold nanoparticles in the TiO₂ film can enhance its tribological performance. Liu et al. found that the TiO₂/5 mol% Au nanocomposites prepared by the sol-gel method demonstrated low friction of 0.09–0.10 against steel balls under the reciprocating friction test [22]. TiO₂/Au decorative thin films fabricated by magnetron sputtering showed a low sliding friction of 0.15 and excellent wear resistance of $2 \times 10^{-6} \text{ mm}^3 \text{ N}^{-1} \text{ m}^{-1}$ after a suitable annealing treatment [23].

Ti6242 has a relatively slow oxidation rate at temperatures up to 700 °C in comparison to CPTi and Ti6Al4V [24,25]; whether this fast CCT works on Ti6242 alloy is still a question that forms the theme of this study. We pre-deposited a thin gold layer on the surface of Ti6242 samples, and CCT was carried out at 640/670/700 °C for 10 or 120 h to investigate if Au can speed up the treatment. After the CCT treatments, the surface and cross-section of the samples were characterized, and the mechanical properties, including hardness, friction, and wear, were evaluated to develop an efficient surface treatment for the Ti6242 alloy to enhance its tribological performance.

2. Materials and Methods

The material used in this project is near alpha Ti-6Al-2Sn-4Zr-2Mo (Ti6242), as shown in Figure 1a. The dark areas are alpha grains, and the light phases are rich in Mo, which are beta phases. The chemical composition of the alloy by atomic percentage is tabulated in the table in Figure 1b. Ti6242 alloy has an elastic modulus of 109–119 GPa and Poisson's ratio of 0.35–0.37. A rod of 32 mm in diameter of Ti6242 was cut and sectioned into 4.5 mm thick coupons using SiC blades by a Metprep cutting machine rotating at 3000 rpm. Then, the coupons were ground progressively from 120, 240, 400, and 800 to 1200 grit before being ultrasonically cleaned in acetone and dried. The gold layer (20–30 nm) was deposited on a prepared Ti6242 sample using a sputtering coater at 25 mA for 6 min.

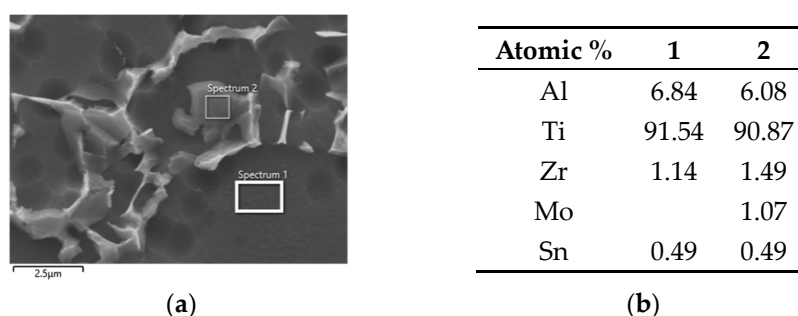


Figure 1. As received Ti-6Al-2Sn-4Zr-2Mo sample: (a) microstructure and (b) composition.

CCT was carried out at the temperatures of 640/670/700 °C for 10 or 120 h in an electric furnace (Elite Thermal Systems Limited, Market Harborough, UK) in the atmosphere with a ramp rate of 8 °C/min and a furnace cooling rate of 2 °C/min. Details of the sample codes and their coatings are listed in Table 1.

Table 1. Sample codes and detailed CCT information.

Code	Pre-Deposition	Temperature (°C)	Duration (h)	Ra (µm)
Untreated	-	-	-	0.067
U640-10	-	640	10	0.068
U640-120	-	640	120	0.069
Au640-120	Au	640	120	0.135
U670-10	-	670	10	0.081
Au670-10	Au	670	10	0.121
U670-120	-	670	120	0.081
Au670-120	Au	670	120	0.082
U700-10	-	700	10	0.086
Au700-10	Au	700	10	0.084

An XP-200 Plus Stylus 3D profilometer was employed to measure the surface roughness (arithmetical mean height, Ra) and plot the profile of the tracks after the tribological tests.

After CCT, the sectioned samples were ground and polished to a mirror-like finish using activated colloidal silica. The cross-section of the sample was etched by Kroll's reagent, comprising 2%HF + 6%HNO₃ + balanced water [26]. A JEOL 7000 scanning electron microscope equipped with an Oxford Aztec energy dispersive X-ray spectroscopy (SEM/EDX, JEOL, Welwyn Garden City, UK) was employed in observing the surface morphology and cross-sectional microstructure, measuring the oxide thickness, collecting elemental information as well as analyzing the wear tracks.

Phase constituents of the samples' surface were identified by a PROTO AXRD benchtop power diffraction system (Proto, Crewe, UK), and the diffraction peaks were identified by an X'Pert HighScore Plus program.

Surface micro-hardness of the untreated and treated samples was measured by a Vickers indenter under a load of 50 g with a holding time of 10 s (Mitutoyo MVK-H1). The distribution of nano-hardness along the depth under the oxide layer was measured by a Micromaterial nano-indenter under a load of 20 mN for 5 s. An ST30 Scratch Tester with a Rockwell spherical cone tip (Teer Coatings Ltd., Droitwich, UK) was used to evaluate the adhesion/cohesion strength of the converted ceramic layers. An initial load of 5 N was applied and increased linearly (10 mm/min) until 60 N.

Tribological properties were tested in a Phoenix TE-79 multi-axis tribology machine. The reciprocating friction and wear test was executed at a sliding speed of 5 mm/s for 1000 cycles over 5 mm under a load of 20 N against a WC ball (8 mm in diameter). Wear track contours were plotted using the 3D profilometer mentioned earlier to calculate the wear areas. Additionally, the morphology and elemental information of the tracks were further examined by SEM and EDX.

3. Results

3.1. Surface Appearance and Morphology

The gold pre-deposited sample demonstrated a light golden color before CCT and took on a dark appearance after CCT, as shown in Figure 2. The surface of the untreated sample turned light yellow-green from a silver metallic color after CCT.

The surface of Ti6242 without a pre-deposited gold layer changed slightly after the CCT treatment, and the grooves left after grinding can still be clearly seen for all the treatments even after 120 h treatment at 670 °C, as demonstrated in Figure 3a. EDX analysis of the composition (Zone 1 in Figure 3a,c) suggested that TiO₂ was formed on the surface. For the gold pre-deposited samples, the grinding mark became blurred after the CCT; there are some particles that can be seen on the surface, as shown in Figure 3b, which are identified as gold agglomerate (Point 2). These particles were evenly distributed on the surface, and they grew larger with increased treatment time and temperature.



Figure 2. Ti6242 samples (a) before and (b) after CCT at 670 °C for 10 h.

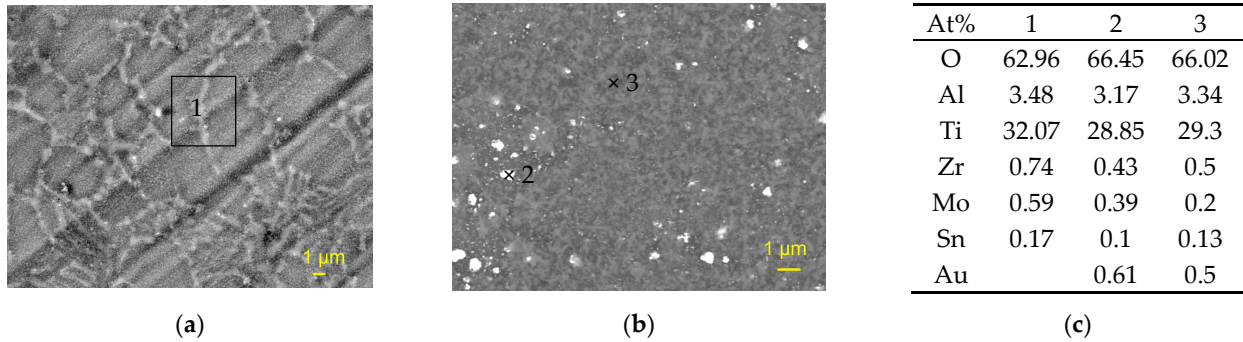


Figure 3. Surface morphology change: (a) U670-120, (b) Au670-120, and (c) EDX composition.

3.2. Cross-Sectional Microstructure

After 10 h CCT, a very thin oxide layer was formed on the surface of the Ti6242 samples. It was only 0.1 μm when treated at 640 °C and increased to 0.2–0.3 μm at 670 °C (Figure 4a) and 0.4–0.6 μm at 700 °C (Figure 4e). Extending the treatment time to 120 h, the oxide layer grew to 0.4–0.5 μm at 640 °C and 0.8–1.0 μm at 670 °C (Figure 4b). With a gold pre-deposited layer, the oxide layer became much thicker after the same CCT. For example, the oxide layer was about 0.5–0.7 μm for Au670-10 (Figure 4b), 1.7–1.9 μm for Au670-120 (Figure 4d), and 0.7–0.8 μm for Au700-10 (Figure 4f).

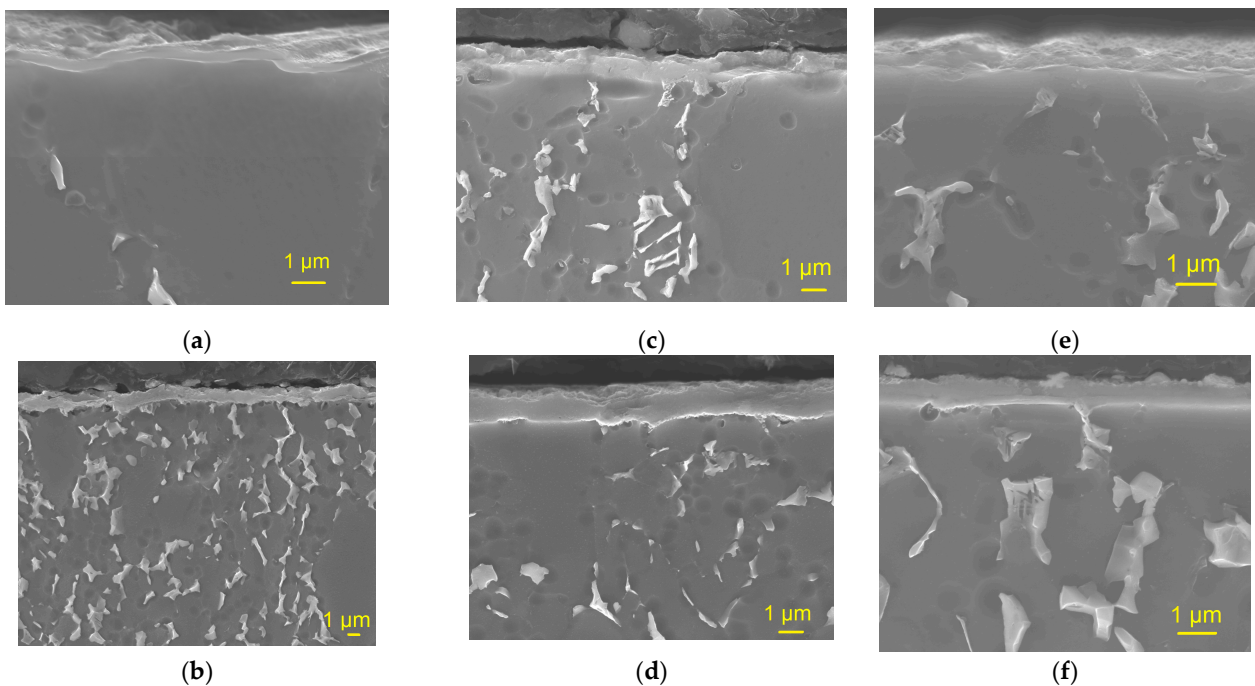


Figure 4. Cross-sectional image of the Ti6242 samples: (a) U670-10, (b) Au670-10, (c) U670-120, (d) Au670-120, (e) U700-10, and (f) Au700-10.

As shown in Figure 5a, less beta phase can be seen under the oxide layer, which is assumed to be an oxygen diffusion zone. Further examination of the cross-sectional backscattering electron image (BEI) of the CCTed samples suggested that gold particles are mainly distributed at the near-surface region of the oxide layer (Figure 5b,c). Most gold particles are nanosized and spread in the oxide layer, while some clusters were also formed, especially at higher temperatures (700 °C/10 h) or longer treatments (670 °C/120 h).

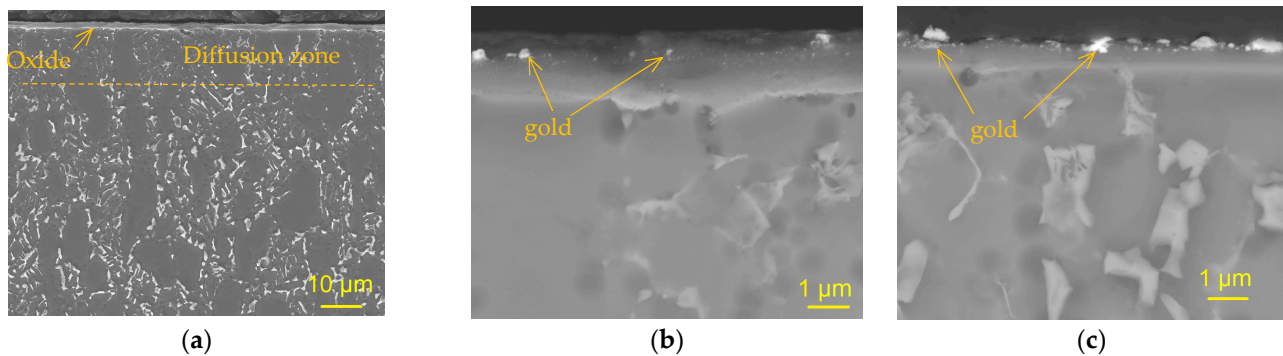


Figure 5. Cross-sectional image of the Ti6242 samples: (a) Au670-120 (SEI), (b) Au670-120 (BEI), and (c) Au700-10.

3.3. Surface Phase Evolution

Ti6242 is mainly composed of alpha phases with a small amount of beta phase, as shown in Figure 6. After CCT, for a short period, oxides started to appear on the surface (U670-10 and U700-10), but alpha phase peaks were still quite strong. After 120-h treatment at 670 °C, both anatase and rutile TiO₂ were formed on the surface, although alpha phases were still detectable. With a gold pre-deposited layer, only rutile TiO₂ can be identified together with alpha phases. The strong alpha phases indicate a shallow oxide layer was formed on the sample.

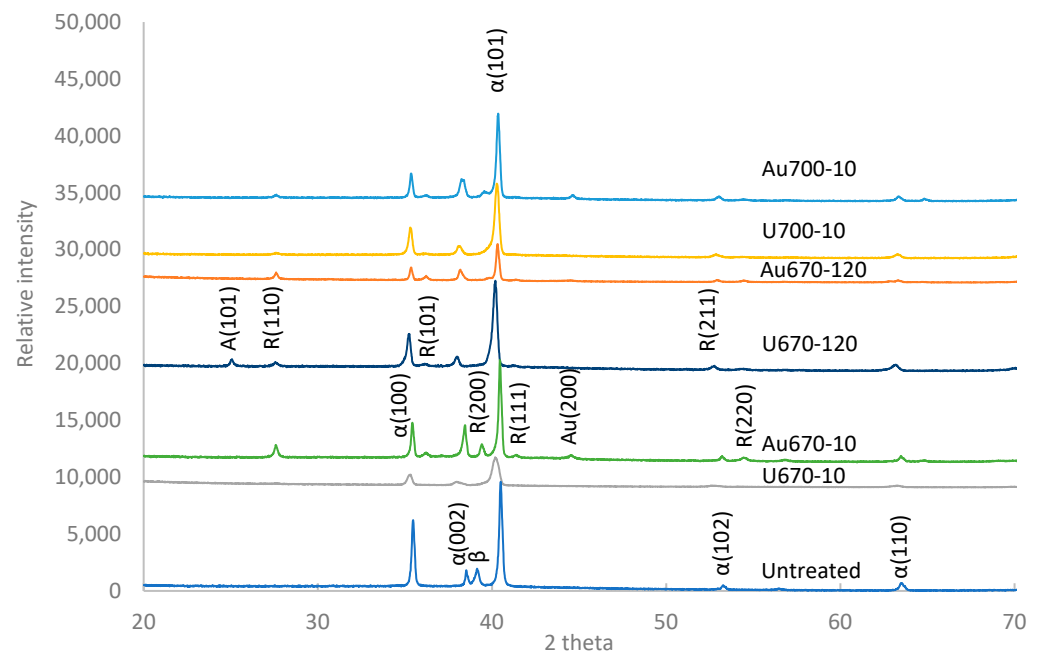


Figure 6. Phase evolution before and after CCT.

3.4. Surface Hardness and Cross-Sectional Hardness Profile

As shown in Figure 7a, all the surfaces became harder after CCT. Untreated Ti6242 had a surface hardness of HV_{0.05}336, and it increased significantly to HV_{0.05}804 after treatment

at 640 °C for 120 h and $HV_{0.05}1045$ after CCT at 670 °C for 120 h. With a gold pre-deposited layer, although the surface hardness value increased, they were slightly lower than those CCTed at the same condition. When treated for a short CCT time of 10 h at 670 °C and 700 °C, the surface hardness increase is smaller than that for long-time (120 h) treated samples. Nanoindentation on the cross-sectional surface helped to define the diffusion zone of oxygen. As displayed in Figure 7b, short-time treatment (10 h) led to a shallow hardened zone (oxygen diffusion zone) even when the temperature was raised to 700 °C, while longer treatment time (120 h) can produce a thick diffusion zone up to 50 μm for both samples with or without gold pre-deposited layer (U670-120 and Au670-120).

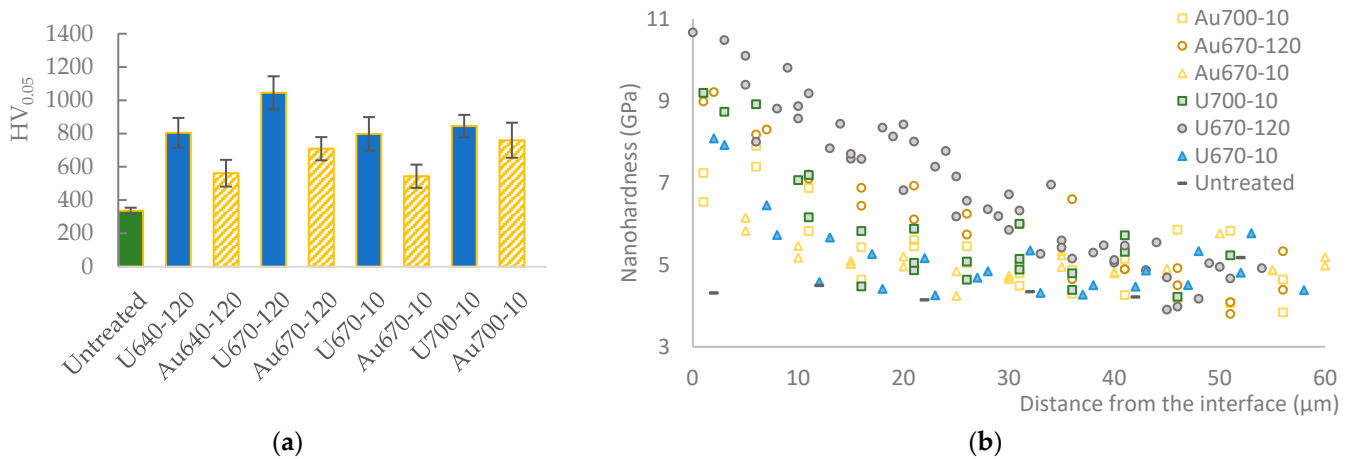


Figure 7. (a) Surface microhardness before and after CCT, (b) cross-sectional nano-hardness profile under the oxide layer.

3.5. Scratch Resistance of the Oxide Layers

As the Rockwell spherical cone tip was applied on the surface of the oxide layer, friction force increased with the load gradually and smoothly for both samples of U670-120 and Au670-10 (Figure 8). The friction force jumped at a load of 45 N for U670-120 and about 50 N for Au670-10. The bottom of the scratch was smooth for the sample Au670-10 but with a lot of transverse cracks for U670-120, indicating the oxide layer was brittle. More chips can be found along the scratch for sample Au670-10, suggesting that there was a brittle superficial layer.

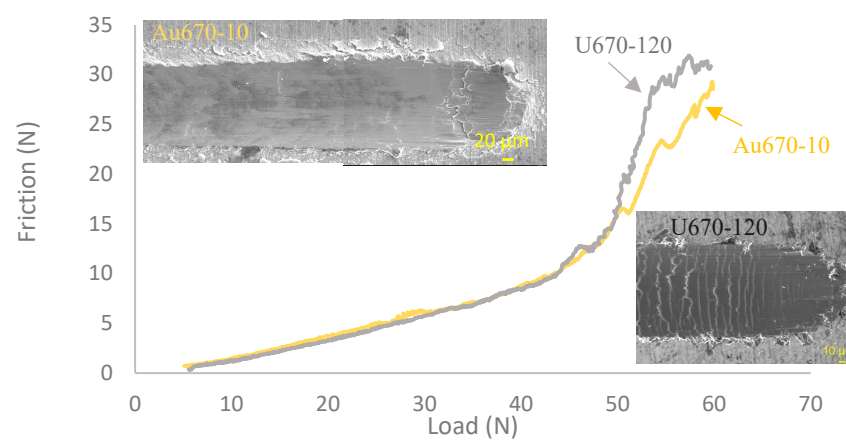


Figure 8. Scratch test on the oxide layer formed on samples U670-120 and Au670-10.

3.6. Tribological Properties

As shown in Figure 9, the Coefficient of Friction (CoF) for the untreated Ti6242 sample started at about 0.4 and fluctuated in the whole test range between 0.2 and 0.5. All the

CCTed samples had a low friction in the beginning. For those samples without a gold pre-deposited layer, the initial CoF was low at about 0.1, and it climbed up quickly after a few tens of cycles. The CoF soared to more than 0.5 after 100 cycles for U640-120 and remained relatively stable until about 800 cycles before escalating further to just under 0.6. The friction for U670-10 rose relatively fast in the first 300 cycles and slowed down until about cycle 800 and then oscillated in a large range between 0.2 and 0.6 in the last 200 cycles. The CoF for U700-10 surged to 0.6 at about cycle 300 and then fluctuated between 0.3 and 0.6 till the end of the test. The CoF of U670-120 climbed steadily in the first 800 cycles before an unstable swinging. The early CoF of gold pre-deposited samples was slightly higher than that of the CCTed samples without gold, but it grew slightly from 0.1–0.2 to 0.2–0.3 and maintained relatively stable in the whole test range, especially for sample Au670-120.

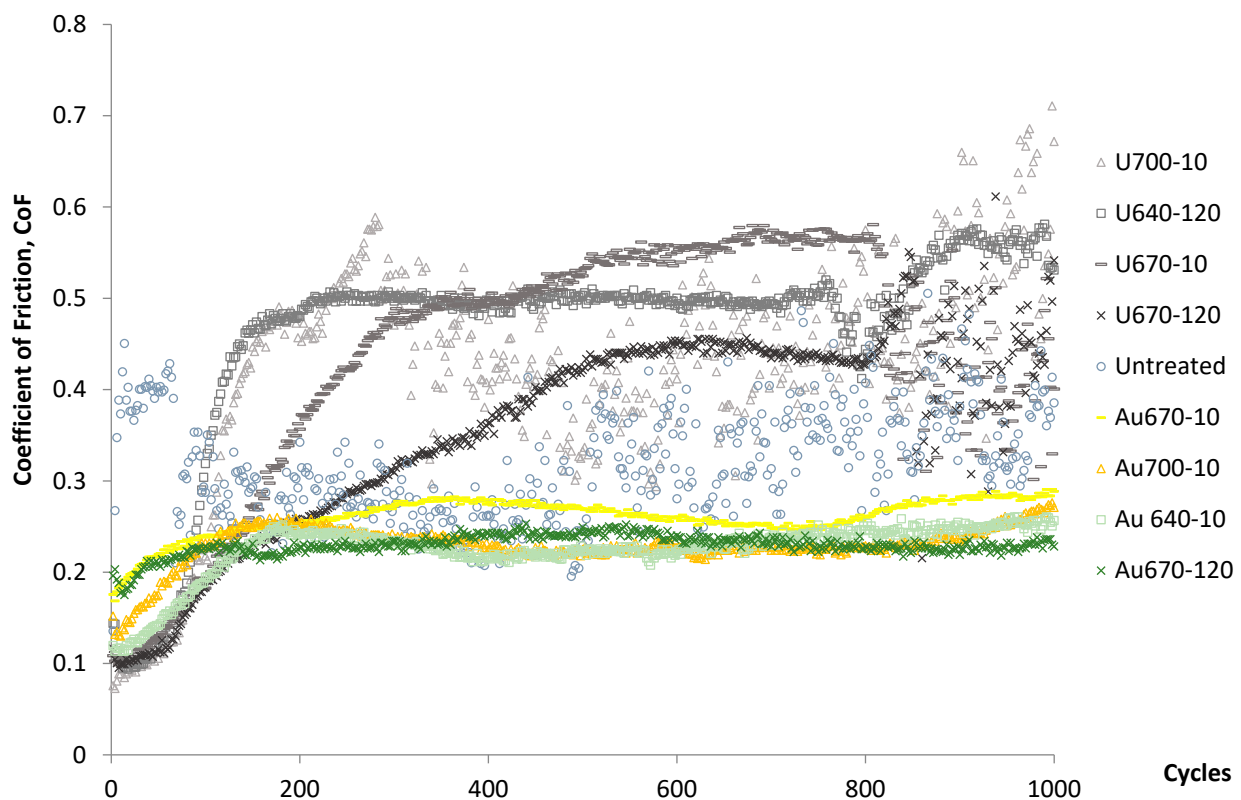


Figure 9. CoF change of the Ti6242 samples against an $\varnothing 8$ mm WC ball.

After the friction test, the wear tracks were plotted by a profilometer, and the representative wear tracks were displayed in Figure 10. After the 1000-cycle reciprocal test, a much wider and deeper track was created for the untreated sample as compared with that for all the CCTed samples. Clear tracks were also scraped on the surface of the samples U670-120 and U700-10. As shown in Figure 11a, deep scuffs were abraded on the surface of sample U700-10, while a crater of similar size was rubbed down on the counterpart WC ball. The surface of the gold pre-deposited sample was only scratched slightly to reveal shallow trails (Figures 10 and 11b).

The wear tracks were analyzed by SEM and EDX, as displayed in Figure 12. Deep abraded grooves, together with adhesive and oxidative areas, were formed on the surface of the untreated sample. An uneven track with grooves and oxide debris particles was formed on sample U670-10, while a very smooth track was formed on sample Au670-10. The composition change in the track is summarized in Table 2.

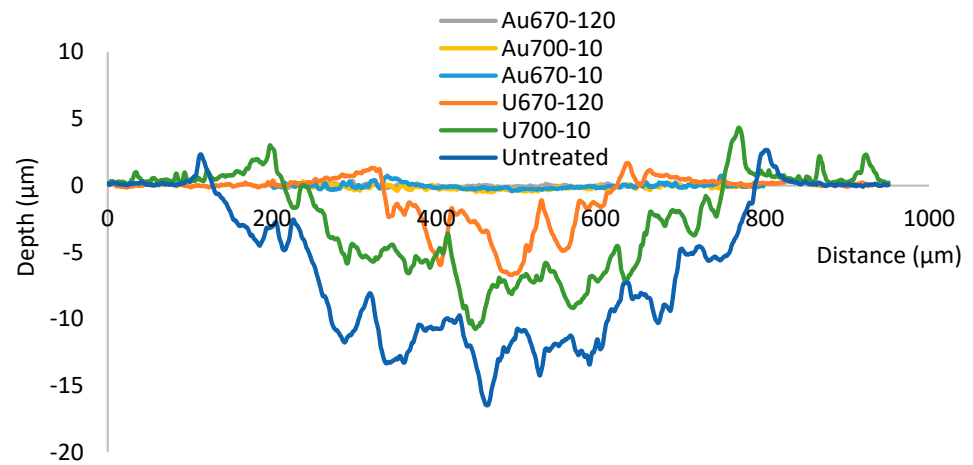


Figure 10. Selected track profile after the tribological test.

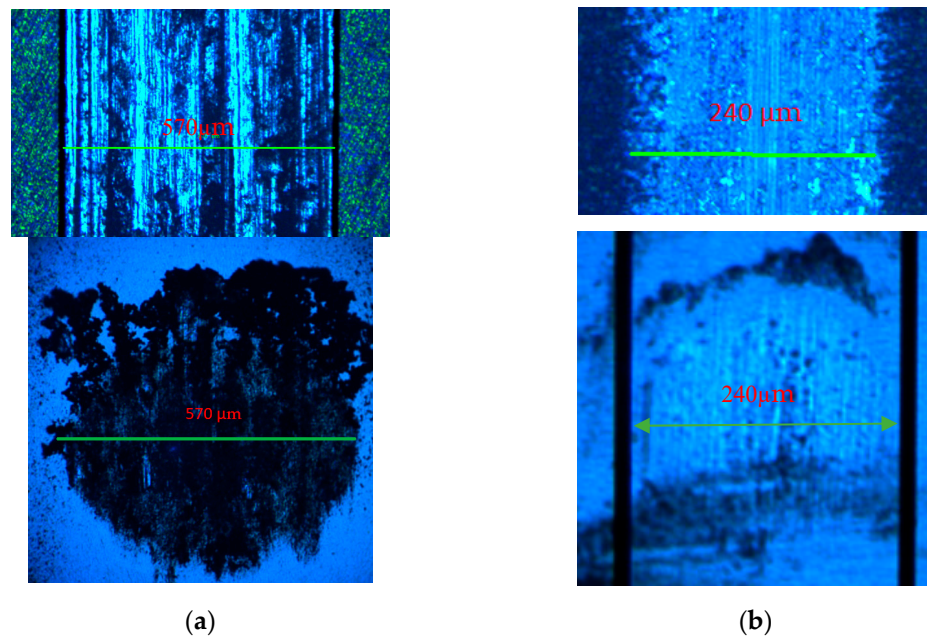


Figure 11. Wear tracks (top) and ball crater (bottom) created in the tribotest: (a) U700-10 and the counterpart ball crater, and (b) Au700-10 and the counterpart ball.

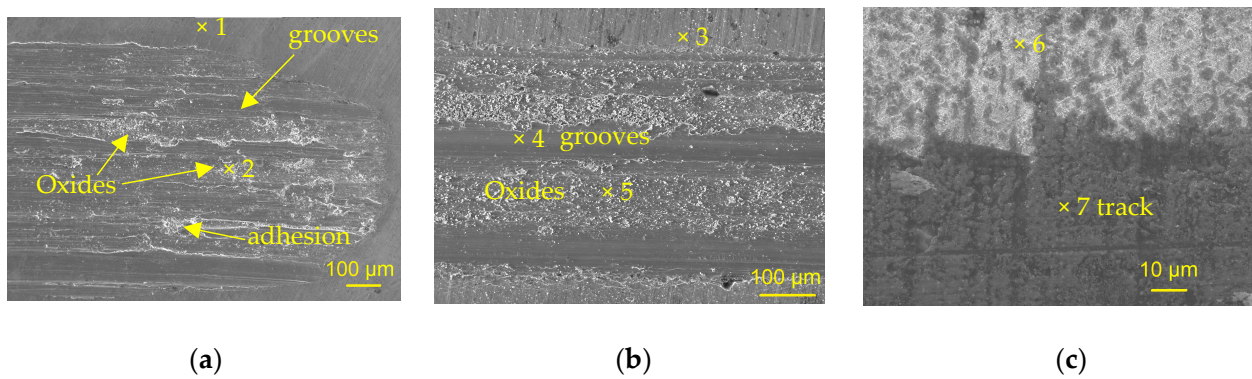


Figure 12. Wear track: (a) untreated, (b) U670-10, and (c) Au670-10.

Table 2. EDX identification of elemental information at different locations of the track.

	Atomic %	O	Al	Ti	Zr	Sn	Mo	W	Au
Untreated	1	1.9	6.61	88.86	1.36	0.5	0.77		
	2	3.87	8.32	86.02	1.16	0.48		0.11	
U670-10	3	5.89	5.98	85.85	1.19		0.61		
	4	14.21	6.18	77.11	1.24	0.48	0.72	0.06	
	5	25.54	5.09	67.97	0.89	0.38		0.13	
Au670-10	6	40.59	3.71	53.01	1.12	0.31	0.55		0.71
	7	39.21	3.64	55.65	0.33	0.27		0.09	0.72

4. Discussion

Titanium alloys oxidize in air at elevated temperatures, which results in the simultaneous formation of an oxide (TiO_2) scale on the surface and an oxygen-rich diffusion zone beneath the scale (Figure 5a), which is due to the high solid solubility of oxygen in α -titanium (i.e., 14.5 wt.% [27]) and high affinity of titanium to absorb oxygen, which instantaneously reacts and stabilizes the α phase. In our previous study, we found that the gold layer on the surface promoted the outward diffusion of Ti atoms to react with oxygen and accelerate the ceramic conversion process, especially at the beginning period [20,28]. Gold has a multi-oxidation state, and the gold atoms are preferentially attached to titanium atoms over oxygen atoms, which assists in the formation of a strongly bonded oxygen/transition-metal system, which can boost their reactivities [29]. In the initial stages, the existence of gold and its high activity greatly increased the titanium atoms' outward diffusion through the clearance among gold particles to react with the incoming activated oxygen atoms and thus resulted in the early increase in the oxidation rate of Ti6242. As the oxide layer grew thicker, the outward diffusion of the titanium atoms became harder, and the inward diffusion of oxygen atoms/molecules dominated the oxidation process which induced a slower oxidation rate. Gold was mainly found in the superficial layer of the oxide, as shown in Figure 5b,c. Gold clusters in oxides had high catalytic activity [30,31]. These clusters and the scattered nanosized gold particles in the superficial layer promote the absorbance and dissociation of oxygen molecules, increasing the oxidation rate. As evidenced in Figure 6, except for sample U670-120, only rutile TiO_2 phases were detectable on the surface, especially for the gold pre-deposited samples. This agreed with the findings of Debeila et al. that gold nanoparticles boosted the transition of anatase to rutile [32].

Compared to Ti-6Al-4V, Ti-6Al-2Sn-4Zr-2Mo alloy presented lower reactivity, and a thinner oxide layer and alpha case were formed on Ti-6242 when isothermally held at 593 °C for 200 h [24]. After 500 h, the thickness of the oxide scale increased to 600 nm, and a 4–5 μm thick oxide layer was formed after 500 h at 700 °C. However, the long treatment time led to a porous oxide layer [25]. The increased oxidation resistance might be due to the addition of alloying elements like Mo or Si, which enhance the oxidation resistance of titanium alloys [33,34].

Oxygen increases the hardness by solid solution strengthening, and the hardness values are directly proportional to the oxygen concentration present in titanium and its alloys [35]. The so-called alpha-case is a continuous and hard layer with high oxygen content, which may affect the mechanical properties of the alloy [36]. As shown in the nano-hardness profile in Figure 7b, the hardness gradually decreased from the surface towards the bulk, and the hard oxygen diffusion zone increased with temperature and treatment time. Similar work was reported for the change in the thickness of the alpha case in the temperature ranges of 500–700 °C for 5–500 h [25].

A wide and deep scuffed track was produced on the untreated Ti6242 sample with the highest wear rate, and the plastically deformed grooves and ridges led to unstable friction (Figures 9–12). This was mainly due to the abrasive ploughing of the hard WC ball into the relatively soft Ti6242 substrate. WC-Co cemented carbide ball has a hardness of HRA 88–90 (equivalent to HV 1100–1200), which is much harder than that of Ti6242 ($\text{HV}_{0.05}336$) [37].

Additionally, delaminated platelets, adhesive material, and oxidative areas were detected in the track (Figure 12a). Heilig et al. found a similar wear mechanism when Ti6242 slid against an AISI E52100 steel ball in a pin-on-disc test [38,39].

The existence of a titanium oxide layer led to a steady CoF for all the CCTed samples, especially at the run-in period due to the hardened surface (Figure 7a). This was because the adherent and compact thin oxide layer decreased the adhesive action of metal/ceramic contact (Ti/WC), notably as a result of the nature of the ceramic/ceramic contact (TiO₂/WC), thus lowering the friction [18]. The maximum Hertzian contact pressure of the WC ball with the untreated Ti6242 was about 1425 MPa, which increased to 2116 MPa for the ceramic-converted surface. Once the oxide layer was cut through, a mixed abrasive and adhesive wear resulted in a sharp rise of CoF, as shown in Figure 9 for all the CCTed samples without gold. A thick layer and hard diffusion zone like U670-120 (Figure 7b) may help delay the increase, but the destruction of the oxide layer and the hard ceramic debris generated in the test led to unstable friction at the end of the test.

Although the initial CoF of the gold pre-deposited and CCTed Ti6242 samples was slightly higher than those CCTed samples without gold, the friction only increased slightly and remained stable till the finish of the test (Figure 9). As shown in Figure 4b,c, the gold particles scattered in the near-surface region after CCT acted as a solid lubricant to reduce the friction in the test. In the end, enough gold particles can still be detected in the track (Figure 12c), suggesting the lasting lubrication of gold in the whole process. Gold particles could self-restore under the applied load thanks to their low shear strength even if a local failure occurred in the TiO₂ layer, therefore decreasing the friction and enhancing the wear resistance in a sliding test [22]. The CoF of the thin TiO₂/Au layer was reduced to 0.16–0.23 against bearing steel in a reciprocating tribotest [23].

Table 3 summarizes the detailed information about all the samples, including surface roughness, oxide layer thickness, the CoF at different stages (cycle 1, 400, and 1000) and the average CoF, the final wear track width, depth, surface area, and the counterpart ball worn crater diameter. The oxide scales formed in the current study are all quite dense and compact as their thickness is lower than 2 μm due to the relatively short treatment time and temperature. For a treatment at a higher temperature, such as 700 °C, the oxide showed poor adherence to the metal substrate after 500 h [25]. Spallation of the oxide layer was also observed in the samples heat-treated at 700 °C for more than 200 h exposure time. Normally, titanium alloys need aging or annealing treatment after working to relieve stress and homogenize the microstructure, and the lower temperature and short treatment duration will avoid the detrimental effect on mechanical properties like fatigue or strength [40]. With the assistance of gold, a 10-h treatment (Au670-10) can generate an oxide layer with better tribological performance than that of the 120-h treatment (U670-120, without any gold pre-deposition) and thus greatly improve the efficiency of ceramic conversion treatment.

Table 3. The statistical data for the tribological test (CoF1 denotes as CoF at Cycle 1).

Sample	Ra (μm)	Oxide Thickness (μm)	Track Width (μm)	Depth (μm)	Area (μm ²)	Ball Crater Diameter (μm)	CoF1	CoF400	CoF1000	Average CoF
Au700-10	0.0841	0.7–0.8	292	0.4358	34.5	238	0.16	0.30	0.35	0.25
U700-10	0.0862	0.4–0.6	578	10.2171	2893.1	590	0.10	0.44	0.70	0.42
Au670-120	0.0821	1.7–1.9	307	0.2407	27.6	239	0.17	0.23	0.23	0.23
U670-120	0.0809	0.7–0.9	336	6.8214	932.4	351	0.15	0.37	0.54	0.36
Au670-10	0.1211	0.5–0.7	282	0.4024	62.9	225	0.18	0.28	0.30	0.26
U670-10	0.0806	0.2–0.3	542	9.5224	2296.8	560	0.11	0.21	0.50	0.44
Au640-120	0.1352	1.3–1.5	321	0.3982	79.3	230	0.11	0.22	0.25	0.22
U640-120	0.0687	0.4–0.5	345	6.543	873.3	353	0.10	0.27	0.41	0.46
Untreated	0.0668	N/A	696	16.0386	5517.9	726.8	0.26	0.32	0.41	0.34

5. Conclusions

In this study, we found that a thin 20–30 nm thick gold layer accelerated the ceramic conversion treatment of Ti6242 alloy significantly at temperatures of 640, 670, and 700 °C, and the thickness of the ceramic oxide layers was almost doubled with the assistance of gold. Gold nanoparticles and clusters were found in the surface region and spread in the oxide layer after CCT. When treated under the same CCT conditions, the surfaces of CCTed Ti6242 without gold pre-deposition were harder than those samples with a pre-deposited gold layer. The oxide layer with gold had a similar adhesion and cohesion in the scratch test. They had low and stable friction and very small wear scars thanks to the hard ceramic TiO₂ layer and the lubrication of incorporated gold nanoparticles and clusters in the dense titanium dioxide layer. By pre-depositing a thin gold layer, the efficiency of the ceramic conversion treatment of Ti6242 alloys improved remarkably.

Author Contributions: Conceptualization, Z.Z.; methodology, Z.Z.; validation, Z.Z., Y.X. and C.L.; formal analysis, Z.Z., Y.X. and C.L.; investigation, Z.Z., Y.X. and C.L.; writing—original draft preparation, Z.Z.; writing—review and editing, Z.Z.; supervision, H.D. All authors have read and agreed to the published version of the manuscript.

Funding: This research received no external funding.

Data Availability Statement: Data are available upon request.

Conflicts of Interest: The authors declare no conflicts of interest.

References

1. Fan, H.; Yang, S. Effects of direct aging on near-alpha Ti-6Al-2Sn-4Zr-2Mo (Ti-6242) titanium alloy fabricated by selective laser melting (SLM). *Mater. Sci. Eng. A* **2020**, *788*, 139533. [[CrossRef](#)]
2. Perumal, A.; Azhagurajan, A.; Baskaran, S.; Prithivirajan, R.; Narayansamy, P. Statistical evaluation and performance analysis of electrical discharge machining (EDM) characteristics of hard Ti-6Al-2Sn-4Zr-2Mo alloy. *Mater. Res. Express* **2019**, *6*, 056552. [[CrossRef](#)]
3. Max, B.; Alexis, J.; Larignon, C.; Perusin, S. Titanium alloy Ti-6242 for high temperature structural application. Static and dynamic mechanical properties and impact of ageing. *MATEC Web Conf.* **2020**, *321*, 11089. [[CrossRef](#)]
4. Galati, M.; Defanti, S.; Saboori, A.; Rizza, G.; Tognoli, E.; Vincenzi, N.; Gatto, A.; Iuliano, L. An investigation on the processing conditions of Ti-6Al-2Sn-4Zr-2Mo by electron beam powder bed fusion: Microstructure, defect distribution, mechanical properties and dimensional accuracy. *Addit. Manuf.* **2022**, *50*, 102564. [[CrossRef](#)]
5. Philip, J.T.; Mathew, J.; Kuriachen, B. Tribology of Ti6Al4V: A review. *Friction* **2019**, *7*, 497–536. [[CrossRef](#)]
6. Fridrici, V.; Fouvry, S.; Kapsa, P. Effect of shot peening on the fretting wear of Ti-6Al-4V. *Wear* **2001**, *250*, 642–649. [[CrossRef](#)]
7. Bacci, T.; Bertamini, L.; Ferrari, F.; Galliano, F.P.; Galvanetto, E. Reactive plasma spraying of titanium in nitrogen containing plasma gas. *Mater. Sci. Eng. A* **2000**, *283*, 189–195. [[CrossRef](#)]
8. Sun, J.; Yao, Q.T.; Zhang, Y.H.; Du, X.D.; Wu, Y.C.; Tong, W.P. Simultaneously improving surface mechanical properties and in vitro biocompatibility of pure titanium via surface mechanical attrition treatment combined with low-temperature plasma nitriding. *Surf. Coat. Technol.* **2017**, *309*, 382–389. [[CrossRef](#)]
9. Bai, X.; Li, J.; Zhu, L. Structure and properties of TiSiN/Cu multilayer coatings deposited on Ti6Al4V prepared by arc ion plating. *Surf. Coat. Technol.* **2019**, *372*, 16–25. [[CrossRef](#)]
10. Movassagh-Alanagh, F.; Abdollah-zadeh, A.; Aliofkhaezraei, M.; Abedi, M. Improving the wear and corrosion resistance of Ti-6Al-4V alloy by deposition of TiSiN nanocomposite coating with pulsed-DC PACVD. *Wear* **2017**, *390–391*, 93–103. [[CrossRef](#)]
11. Wan, Y.Z.; Raman, S.; He, F.; Huang, Y. Surface modification of medical metals by ion implantation of silver and copper. *Vacuum* **2007**, *81*, 1114–1118. [[CrossRef](#)]
12. Khan, I. Improving the Cytocompatibility and Infection, Wear and Corrosion Resistances of Commercially Pure Titanium by Laser Micropatterning and Ceramic Conversion Treatment. Ph.D. Thesis, The University of Birmingham, Birmingham, UK, 2020.
13. Zhang, L.-C.; Chen, L.-Y.; Wang, L. Surface Modification of Titanium and Titanium Alloys: Technologies, Developments, and Future Interests. *Adv. Eng. Mater.* **2020**, *22*, 1901258. [[CrossRef](#)]
14. Gao, K.; Zhang, Y.; Yi, J.; Dong, F.; Chen, P. Overview of Surface Modification Techniques for Titanium Alloys in Modern Material Science: A Comprehensive Analysis. *Coatings* **2024**, *14*, 14010148. [[CrossRef](#)]
15. Acar, M.T.; Kovacı, H.; Çelik, A. Enhancement of the tribological performance and surface wettability of Ti6Al4V biomedical alloy with boric/sulfuric acid anodic film. *Surf. Topogr. Metrol. Prop.* **2021**, *9*, 035024. [[CrossRef](#)]
16. Yetim, A.F. Investigation of wear behavior of titanium oxide films, produced by anodic oxidation, on commercially pure titanium in vacuum conditions. *Surf. Coat. Technol.* **2010**, *205*, 1757–1763. [[CrossRef](#)]

17. Fattah-alhosseini, A.; Molaei, M. A review of functionalizing plasma electrolytic oxidation (PEO) coatings on titanium substrates with laser surface treatments. *Appl. Surf. Sci. Adv.* **2023**, *18*, 100506. [[CrossRef](#)]
18. Dong, H.; Bell, T. Enhanced wear resistance of titanium surfaces by a new thermal oxidation treatment. *Wear* **2000**, *238*, 131–137. [[CrossRef](#)]
19. Zhang, Z.; Zhang, Y.; Tao, X.; Liu, K.; Burns, A.; Li, P.; Mukinay, T.; Li, X.; Dong, H. The exceptional oxidation of Ti6Al4V alloy with a pre-deposited silver layer. *J. Alloys Compd.* **2022**, *901*, 163574. [[CrossRef](#)]
20. Zhang, Z.; Yu, H.; Li, X.; Dong, H. Impact of the Amount of the Gold Layer on the Tribological Performance of the Ceramic Conversion Treated CP-Titanium. *Tribol. Lett.* **2023**, *71*, 36. [[CrossRef](#)]
21. Antler, M.; Spalvins, T. Lubrication with thin gold films. *Gold Bull.* **1988**, *21*, 59–68. [[CrossRef](#)]
22. Liu, W.-m.; Chen, Y.-x.; Kou, G.-T.; Xu, T.; Sun, D.C. Characterization and mechanical/tribological properties of nano Au–TiO₂ composite thin films prepared by a sol–gel process. *Wear* **2003**, *254*, 994–1000. [[CrossRef](#)]
23. Abreu, C.S.; Matos, J.; Cavaleiro, A.; Alves, E.; Barradas, N.P.; Vaz, F.; Torrell, M.; Gomes, J.R. Tribological characterization of TiO₂/Au decorative thin films obtained by PVD magnetron sputtering technology. *Wear* **2015**, *330–331*, 419–428. [[CrossRef](#)]
24. Gaddam, R.; Sefer, B.; Pederson, R.; Antti, M.L. Study of alpha-case depth in Ti-6Al-2Sn-4Zr-2Mo and Ti-6Al-4V. *IOP Conf. Ser. Mater. Sci. Eng.* **2013**, *48*, 12002. [[CrossRef](#)]
25. Gaddam, R.; Sefer, B.; Pederson, R.; Antti, M.-L. Oxidation and alpha-case formation in Ti-6Al-2Sn-4Zr-2Mo alloy. *Mater. Charact.* **2015**, *99*, 166–174. [[CrossRef](#)]
26. Pace Technologies. Metallographic Etchants. Available online: <https://www.metallographic.com/Metallographic-Etchants/Metallography-Etchants.htm> (accessed on 13 March 2024).
27. Murray, J.; Wriedt, H. *Binary Alloy Phase Diagrams*; Massalski, T.B., Ed.; ASM International: Geauga County, OH, USA, 1990; p. 2924.
28. Zhang, Z.; Zhang, Y.; Li, X.; Alexander, J.; Dong, H. An enhanced ceramic conversion treatment of Ti6Al4V alloy surface by a pre-deposited thin gold layer. *J. Alloys Compd.* **2020**, *844*, 155867. [[CrossRef](#)]
29. Hutchings, G.J. Selective oxidation using supported gold bimetallic and trimetallic nanoparticles. *Catal. Today* **2014**, *238*, 69–73. [[CrossRef](#)]
30. Chen, M.S.; Goodman, D.W. The structure of catalytically active gold on titania. *Science* **2004**, *306*, 252–255. [[CrossRef](#)] [[PubMed](#)]
31. Busiakiewicz, A.; Kisielevska, A.; Piwoński, I.; Batory, D.; Pabianek, K. Formation of gold and platinum nanostructures on rutile TiO₂(001) by thermal treatment of thin films in vacuum. *Vacuum* **2019**, *163*, 248–254. [[CrossRef](#)]
32. Debeila, M.A.; Raphulu, M.C.; Mokoena, E.; Avalos, M.; Petranovskii, V.; Coville, N.J.; Scurrrell, M.S. The effect of gold on the phase transitions of titania. *Mater. Sci. Eng. A* **2005**, *396*, 61–69. [[CrossRef](#)]
33. Berthaud, M.; Popa, I.; Chassagnon, R.; Heintz, O.; Lavková, J.; Chevalier, S. Study of titanium alloy Ti6242S oxidation behaviour in air at 560 °C: Effect of oxygen dissolution on lattice parameters. *Corros. Sci.* **2020**, *164*, 108049. [[CrossRef](#)]
34. Shree Meenakshi, K.; Ananda Kumar, S. Corrosion resistant behaviour of titanium–Molybdenum alloy in sulphuric acid environment. *Mater. Today Proc.* **2022**, *65*, 3282–3287. [[CrossRef](#)]
35. Rosa, C.J. Oxygen diffusion in alpha and beta titanium in the temperature range of 932° to 1142 °C. *Metall. Trans.* **1970**, *1*, 2517–2522. [[CrossRef](#)]
36. Wagner, L.; Wollmann, M. Titanium and Titanium Alloys. *Struct. Mater. Process. Transp.* **2013**, 151–180.
37. He, M.; Wang, J.; He, R.; Yang, H.; Ruan, J. Effect of cobalt content on the microstructure and mechanical properties of coarse grained WC-Co cemented carbides fabricated from chemically coated composite powder. *J. Alloys Compd.* **2018**, *766*, 556–563. [[CrossRef](#)]
38. Heilig, S.; Ramezani, M.; Neitzert, T.; Liewald, M. Tribological Performance of Duplex-Annealed Ti-6Al-2Sn-4Zr-2Mo Titanium Alloy at Elevated Temperatures Under Dry Sliding Condition. *J. Mater. Eng. Perform.* **2018**, *27*, 2003–2009. [[CrossRef](#)]
39. Heilig, S.; Ramezani, M.; Neitzert, T.; Liewald, M. Investigation of Friction and Wear Properties of Duplex-Annealed Ti-6Al-2Sn-4Zr-2Mo Against Hardened AISI E52100 at Linear Reciprocating Motion. *Trans. Indian Inst. Met.* **2018**, *71*, 1257–1264. [[CrossRef](#)]
40. Matthew, J.; Donachie, J. *Titanium, A Technical Guide*, 2nd ed.; ASM International, The Materials Information Society: Geauga County, OH, USA, 2000; p. 380.

Disclaimer/Publisher’s Note: The statements, opinions and data contained in all publications are solely those of the individual author(s) and contributor(s) and not of MDPI and/or the editor(s). MDPI and/or the editor(s) disclaim responsibility for any injury to people or property resulting from any ideas, methods, instructions or products referred to in the content.